fluorenylidene adduct **methyl 8(*S*)-acetyl-9(*S*)-(fluoren-9-ylidenemethyl)-12(*S*)-hydroxy-5(*Z*),10(*E*)-heptadecadienoate (34SR)**: ^{1}H NMR δ 7.91 (dd, H, *J* = 6.7, 1.6 Hz, aromatic), 7.76–7.60 (3 H, aromatic), 7.42–7.20 (4 H, aromatic), 6.46 (d, H, *J* = 10.2 Hz), 5.76–5.51 (2 H, C-10, C-11 H's), 5.42–5.20 (2 H, C-5, C-6 H's), 4.22 (ddd, H, *J* = 5.8, 9.6, 10.2 Hz, C-9 H), 4.02 (apparent q, H, *J* = 5.4 Hz, C-12 H), 3.58 (s, 3 H, OCH_3), 2.85 (ddd, H, *J* = 4.6, 9.3, 9.6 Hz, C-8 H), 2.47–2.18 (2 H, C-7 H), 2.17 (t, 2 H, *J* = 7.3 Hz, C-2 H), 2.15 (s, 3 H, acetyl methyl), 1.91 (apparent q, 2 H, *J* = 7.8 Hz, C-4 H), 1.54 (apparent quintet, 2 H, *J* = 7.2 Hz, C-3 H), 1.53 (br, H, OH), 1.48–1.30 (2 H, C-13 H), 1.22 (br s, 6 H, C-14, C-15, C-16 H's), 0.83 (t, 3 H, *J* = 6.4 Hz, C-17 H); UV (c 4.38 × 10^{-5}, n-hexane) [λ(ε)], 314 (13 200), 301 (12 900), 285 (15 000), 282 (shoulder) (13 700), 257 (40 000), 248 (30 300), 229 (39 300).

Consecutive Hydrolysis and Oxidative Cleavage of 25SS. The procedure was the same as that used for the C-8(*R*),C-9(*R*) diastereomer **25RR** described above, except the acidic deprotection and oxidative cleavage was performed on **25SS** (53.2 mg, 0.096 mmol) derived from isopropylidene-D-glyceraldehyde (**14R**). This afforded 34.5 mg (98% material balance) of a light yellow oil. Analysis of this oil by ^{1}H NMR spectroscopy indicated[32] that the product was a mixture containing at least 65% of **methyl 8-(*S*)-acetyl-9(*S*)-formyl-12(*S*)-hydroxy-5(*Z*),10(*E*)-heptadecadienoate (29SS)**: ^{1}H NMR δ 9.46 (s, H, CHO), 5.75 (dd, H, *J* = 15.5, 6.2 Hz, C-11 H), 5.59–5.17 (4 H, OH, C-5, C-6, C-10 H's), 4.09 (apparent q, H, *J* = 5.3 Hz, C-12 H), 3.63 (s, 3 H, OCH_3), 3.49 (dd, H, *J* = 9.5, 9.9 Hz, C-9 H), 2.95 (ddd, H, *J* = 10.0, 7.9, 4.4 Hz, C-8 H), 2.37–1.97 (2 H, C-7 H), 2.26 (t, 2 H, *J* = 7.1 Hz, C-2 H), 2.21 (s, 3 H, acetyl methyl), 2.02 (apparent q, 2 H, *J* = 7.5 Hz, C-4 H), 1.63 (apparent quintet, 2 H, *J* = 7.5 Hz, C-3 H), 1.52–1.34 (2 H, C-13 H), 1.25 (br s, 6 H, C-14, C-15, C-16 H's), 0.84 (t, 3 H, *J* = 6.7 Hz, C-17 H) (a minor aldehydic proton resonance was also observed at δ 9.55 which was tentatively assigned to the C-8 epimer **29RS**; this epimer accounted for less than 5% of the mixture); ^{13}C NMR δ 210.90 (acetyl carbonyl), 199.68 (formyl carbonyl), 174.17 (C-1), 141.80 (C-11), 131.58, 125.64, 122.02, 72.19 (C-12), 57.19, 51.55, 51.12, 37.10, 33.16, 31.61, 30.91, 27.04, 26.48, 25.02, 24.48, 22.51, 13.95 (C-17). This product mixture was further characterized by conversion of the aldehydes to stable adducts by reaction with 9-fluorenylidenetri-*n*-butylphosphorane (**33**).[20] Thus, to a solution of the aldehyde [2 mg (60% purity), 3 μmol] in 300 μL of dry $CDCl_3$ was added 200 μL of a 0.27 M solution of fluorenylidenetri-*n*-butylphosphorane (**33**) in $CDCl_3$. The reaction was followed by the disappearance of the major aldehyde signal (δ 9.46) in the ^{1}H NMR spectrum. The workup and purification of the major Wittig adduct **34SS** was performed exactly as described above for **34RR**. This afforded 1.1 mg (2 μmol, 70% yield) of **methyl 8(*S*)-acetyl-9(*R*)-(fluoren-9-ylidenemethyl)-12(*S*)-hydroxy-5,10-heptadecadienoate (34SS)**: ^{1}H NMR δ 7.89 (dd, H, *J* = 6.5, 1.7 Hz aromatic), 7.70–7.61 (3 H, aromatic), 7.40–7.20 (4 H, aromatic), 6.55 (d, H, *J* = 10.1 Hz), 5.81–5.59 (2 H, C-10, C-11 H's), 5.47–5.23 (2 H, C-5, C-6 H's), 4.23–4.12 (m, H, C-9 H), 4.08 (apparent q, H, *J* = 5.7 Hz, C-12 H), 3.64 (s, 3 H, OCH_3), 2.80 (dt, H, *J* = 8.7, 5.8 Hz, C-8 H), 2.47–2.35 (2 H, C-7 H), 2.24 (t, 2 H, *J* = 7.2 Hz, C-2 H), 2.07 (s, 3 H, acetyl methyl), 2.02 (apparent q, 2 H, *J* = 7.2 Hz, C-4 H), 1.60 (apparent quintet, 2 H, *J* = 7.4 Hz, C-3 H), 1.55 (br, H, OH), 1.53–1.36 (2 H, C-13 H), 1.19 (br s, 6 H, C-14, C-15, C-16 H's), 0.78 (t, 3 H, *J* = 5.3 Hz, C-17 H); UV (*c* 2.73 × 10^{-5}, *n*-hexane) [λ(ε)], 313 (12 600), 300 (12 200), 284 (14 000), 279 (shoulder) (13 300), 258 (40 700), 249 (28 700), 229 (37 000).

Acknowledgment. We thank the National Institute of General Medical Sciences of the National Institutes of Health for support of this research by Grant GM21249-12.

Decomposition of Levuglandin E_2. Dehydration and Allylic Rearrangement Products[1]

Rajkumar S. Iyer, Donald B. Miller, and Robert G. Salomon*

Department of Chemistry, Case Western Reserve University, Cleveland, Ohio 44106

Received September 5, 1989

In aqueous solutions at 37 °C the β,γ-unsaturated δ-hydroxy aldehyde functional array in levuglandin E_2 (LGE_2) readily eliminates water to give an α,β,γ,δ-unsaturated aldehyde, anhydro levuglandin E_2 ($AnLGE_2$), in competition with allylic prototropic shift to give an α,β-unsaturated δ-hydroxy aldehyde, Δ^9-LGE_2. The allylic isomerization is catalyzed by $H_2PO_4^-$, perhaps by a bifunctional mechanism involving both proton acceptance by and donation from the catalyst. Thus, by appropriate adjustment of buffer *concentration*, the product distribution can be altered in a synthetically useful manner. Unexpectedly, the dehydration is *not* catalyzed by acid under the conditions examined (pH 2.8–8.0) and LGE_2 is *most* stable at pH 3–4.

Introduction

The complexity of the arachidonic acid (AA) cascade and of its myriad involvements in normal and pathophysiological processes is widely recognized. Recently we discovered a new branch in the cyclooxygenase pathway of the AA cascade, the formation of levuglandins.[2] Thus, decomposition of the prostaglandin endoperoxide PGH_2 under the aqueous conditions of its biosynthesis produces two levulinaldehyde derivatives, LGE_2 and LGD_2, concomitantly with the corresponding[3] prostaglandins PGE_2 and PGD_2. The fact that these primary levuglandins are themselves susceptible to facile molecular transformations, i.e. dehydration and rearrangement, further complicates studies of the cyclooxygenase pathway. As a foundation for investigations on the biochemistry of levuglandins, a thorough understanding of their chemical reactions is desirable especially in view of the biological activities of

(1) Paper 26 in the series Prostaglandin Endoperoxides. For paper 25, see: Miller, D. B.; Raychaudhuri, S. R.; Avasthi, K.; Lal, K.; Levison, B.; Salomon, R. G. *J. Org. Chem.*, preceding paper in this issue.

(2) (a) Zagorski, M. G.; Salomon, R. G. *J. Am. Chem. Soc.* **1982**, *104*, 3498. (b) Zagorski, M. G.; Salomon, R. G. *J. Am. Chem. Soc.* **1984**, *106*, 1750. (c) Salomon, R. G.; Miller, D. B.; Zagorski, M. G.; Coughlin, D. J. *J. Am. Chem. Soc.* **1984**, *106*, 6049.

(3) *Formally*, PGE_2 and LGE_2 are interconvertable by aldol condensation as are PGD_2 and LGD_2. This interconversion has never been detected.

0022-3263/90/1955-3175$02.50/0

Chart I

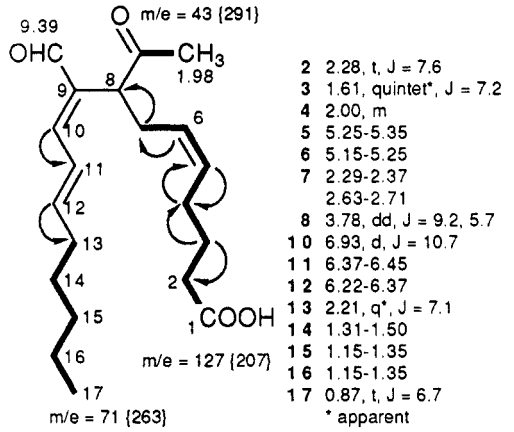

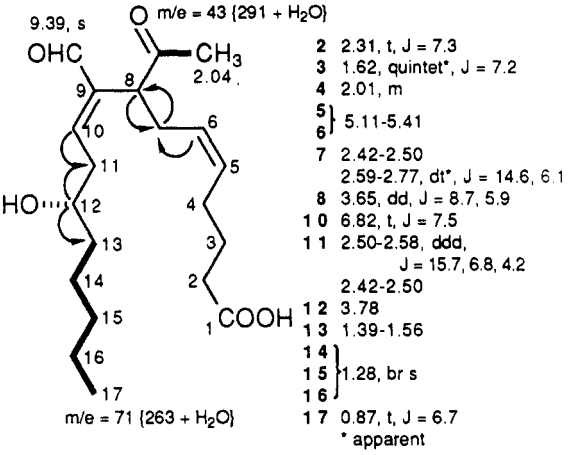

the dehydration products.[4] The dehydration and allylic rearrangement reactions of LGE_2 in aqueous solutions are now examined from pH 3 to pH 8.

Results and Discussion

Characterization of the Products. Dehydration of LGE_2 (1) transpired cleanly upon standing in solution at room temperature for 2 days in 0.01 M aqueous pH 7.8 sodium phosphate buffer. Pure $AnLGE_2$ (2) was obtained in 86% yield by HPLC. In contrast with 1, the dienal 2

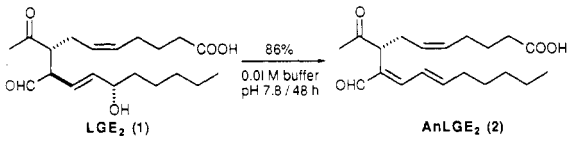

is intensely UV active, λ_{max} = 286 (ϵ = 20900; $CDCl_3$). Both ^{13}C (20 resonances) and ^1H (Chart I) NMR spectra suggest that 2 is a single isomer. Homonuclear decoupling experiments, designated by arrows, confirmed the assignments presented in Chart I for the hydrogen resonances of 2. An *E* configuration for the 9,10-C=C bond is indicated by the appearance of only one vinyl hydrogen resonance below δ 6.9. The resonances for two vinyl hydrogens, i.e. those at positions 10 and 11, would be expected[5] to occur downfield of δ 6.9 if the 9,10-C=C bond had a *Z* configuration. The mass spectrum of 2 shows a base peak at *m/e* = 43, which corresponds to H_3CCO^+, an ion characteristic of levuglandins not found in the mass spectra of any other cyclooxygenase metabolite. The remaining $C_{18}H_{27}O_3$ counter fragment (*m/e* = 291) also appears in the spectrum. Peaks corresponding to the C13–C17 pentyl (C_5H_{11} at *m/e* 71) and C1–C7 carboxyheptenyl ($C_7H_{11}O_2$ at *m/e* = 127) fragments as well as their counter fragments at *m/e* = 263 ($C_{15}H_{19}O_4$) and 207 ($C_{13}H_{19}O_2$) are also prominent.

In contrast with the above reaction *in 0.01 M aqueous pH 7.8 sodium phosphate buffer*, LGE_2 (1) was transformed into an almost 1:1 mixture of two products upon standing in solution at room temperature for 2 days *in 0.1 M aqueous pH 7.8 sodium phosphate buffer*. Besides the dehydration product 2, an allylic rearrangement product, Δ^9-LGE_2 (3), was also formed. A control experiment (in 0.1 M aqueous pH 7.8 sodium phosphate buffer, see the Experimental Section) demonstrated that dehydration of

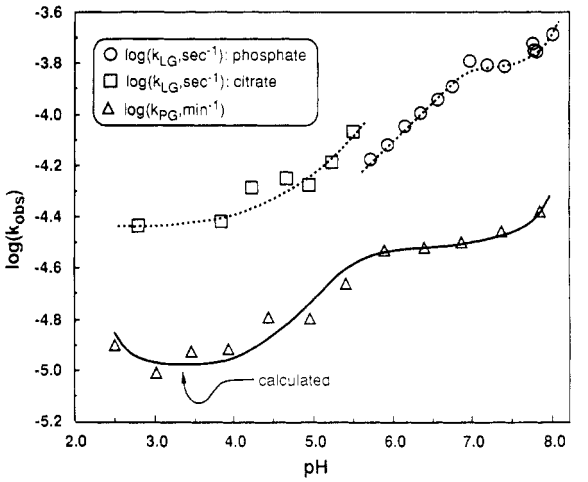

Figure 1. Logarithm of rate constant (k_{obs}) for disappearance of LGE_2 (□ and ○) at 37 °C and PGE_2 (△, data from ref 6) at 25 °C versus pH.

3 is slow under these reaction conditions and that therefore 3 is not an intermediate in the dehydration of 1 to give 2.

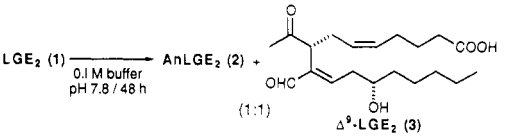

The conjugated enone 3 is moderately UV active, λ_{max} = 215.5 (ϵ = 6000; $CDCl_3$). Both ^{13}C (20 resonances) and ^1H (Chart I) NMR spectra suggest that 3 is a single isomer. Homonuclear decoupling experiments, designated by arrows, confirmed the assignments presented in Chart I for the hydrogen resonances of 3. An *E* configuration for the 9,10-C=C bond is presumed for 3 by analogy with 2. As for 2, the mass spectrum of 3 shows a C_2H_3O base peak at *m/e* = 43 and a $C_{18}H_{27}O_3$ fragment (*m/e* = 291) corresponding to loss of H_2O and C_2H_3O. A peak corresponding to the C13–C17 pentyl (C_5H_{11}, *m/e* 71) and a $C_{15}H_{19}O_4$ fragment (*m/e* = 263) corresponding to the loss of H_2O and C_5H_{11} are also prominent.

Kinetic Studies. The rate constant, k_{obs}, for disappearance of LGE_2 was determined as a function of pH by spectroscopically monitoring the appearance of UV-active products at 232 and 292 nm, the λ_{max} for Δ^9-LGE_2 (3) and $AnLGE_2$ (2), respectively (Figure 1). In 0.1 M pH 2.8–4.8 citrate–phosphate buffer, disappearance is slowest ($t_{1/2}$ = 310 min) under acidic conditions being nearly pH independent below pH 4. At higher hydrogen ion concentration log (k_{obs}) increases linearly with pH. A good linear

(4) (a) Foreman, D.; Zuk, L.; Miller, D. B.; Salomon, R. G. *Prostaglandins* **1987**, *34*, 91. (b) Foreman, D.; Levison, B. S.; Miller, D. B.; Salomon, R. G. *Prostaglandins* **1988**, *35*, 115.

(5) Ananthasubramanian, L.; Carey, S. T.; Nair, M. S. R. *Tetrahedron Lett.* **1978**, 3527 and references cited therein.

correlation (R^2 = 0.977), log (k_{obs}) = 0.27pH − 5.7, is also found in 0.1 M phosphate buffer between pH 5.7 and 7.0. The rate of disappearance continues to rise with increasing pH, albeit more slowly at first, reaching $t_{1/2}$ = 56 min at pH 8. Since the rate generally decreases as [H^+] increases, acid catalysis is not a dominant factor for the decomposition of LGE_2 under the conditions examined (pH 2.8–8.0). In fact, in this pH range *aqueous solutions of levuglandin E_2 are most stable at lower pH.* It is noteworthy that similar behavior was noted[6] for the pH dependence of log (k_{obs}) in the decomposition of PGE_2 for which "maximum stability is obtained at ca. pH 3–4"[7] in aqueous solution. The decomposition of this prostaglandin produces PGA_2 by dehydration of the β-hydroxy carbonyl array, most likely by an E1cB mechanism involving rate-determining generation of an enol or enolate of the ketone carbonyl. Also presented in Figure 1 is the kinetic data[6] for PGE_2 together with the curve[6] generated assuming that first-order PGE_2 degradation can be described empirically by eq 1. Specific base catalysis of PGE_2 dehydration owing

$$-\frac{d[PGE_2]}{dt} = k_{H_3O^+}[H^+] + k_{OH^-}[OH^-] + k_{H_2O}[H_2O] + k_{RCOO^-}[RCOO^-]_{effective}[PGE_2] \quad (1)$$

to the increasing importance of the $k_{OH^-}[OH^-]$ term in eq 1 is evidenced by the rapidly accelerating rate above pH 7.5. A similar rate acceleration with increasing pH is apparent in the log (k_{obs}) versus pH curve for LGE_2 disappearance above pH 7.5 (see top curve in Figure 1).

The last term in eq 1 takes into account a presumed intramolecular general base catalysis by the carboxylate anion of enol–enolate formation leading to dehydration of PGE_2.[6] Consistent with this hypothesis is the occurrence of an inflection point at about pH 5 in the pH dependence for log (k_{obs}) for PGE_2 corresponding to the pK_a of the carboxylic acid functionality in the prostaglandin.[7] Further evidence for intramolecular general base catalysis was provided by comparisons of the dehydration rate constant for PGE_2 with that of an ester for which carboxylate catalysis is precluded.[8] Removing the influence of the carboxyl group by esterification has no apparent effect on the rate constant at pH 4.0, suggesting no involvement of intramolecular general acid catalysis by the carboxyl group. But, at pH 6, where PGE_2 exists mainly as the carboxylate anion, the acid shows a significant increase in dehydration rate, $k_{obs} = 0.63 \times 10^{-4}$ s^{-1}, relative to the ester, 0.43×10^{-4} s^{-1}. Intramolecular proton abstraction leading to enolate generation accelerates the decomposition because the *effective* concentration of the base, i.e. the carboxylate anion, is several orders of magnitude greater than the bulk concentration of the prostaglandin itself.

An inflection point in the vicinity of pH 5 is also apparent in the log (k_{obs}) versus pH data for LGE_2 (Figure 1). To test the possibility that decomposition of LGE_2 can be induced intramolecularly by the carboxylate group, the rates of decomposition of LGE_2 and LGE_2 methyl ester were compared at pH 8.2 where the levuglandin exists mainly as the carboxylate anion. To assure solubility of the ester, an 0.1 M phosphate buffer was prepared in 75% aqueous acetonitrile. In this buffer, the rate of decomposition of LGE_2, $k_{obs} = (2.31 \pm 0.05) \times 10^{-4}$ s^{-1}, is significantly elevated relative to that of its methyl ester, $k_{obs} = (0.55 \pm 0.16) \times 10^{-4}$ s^{-1}. Intramolecular catalysis by the carboxylate anion might involve abstraction of a proton

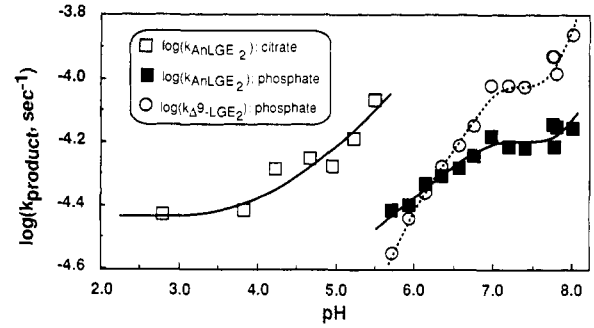

Figure 2. Logarithm of rate constants for appearance of $AnLGE_2$ (**2**) and Δ^9-LGE_2 (**3**) as a function of pH at 37 °C in aqueous 0.1 M buffer solutions: (□) citrate–phosphate, (○ and ■) phosphate.

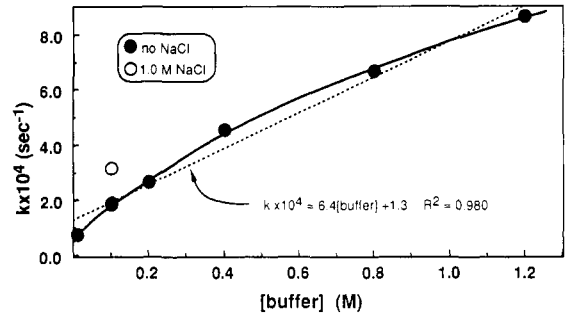

Figure 3. Rate constant for disappearance of LGE_2 (**1**) as a function of pH 7.75 ± 0.05 phosphate buffer concentration at 37 °C.

α to the aldehyde leading directly to dehydration as depicted in **4** or leading to enolate generation as depicted in **5**.

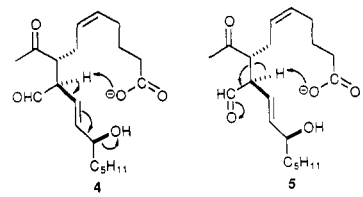

4 **5**

The decomposition of LGE_2 is a complex process generating not only a dehydration product, $AnLGE_2$ (**2**), but also a product from allylic rearrangement of the 10–11 C=C bond, the conjugated 9,10-unsaturated aldehyde Δ^9-LGE_2 (**3**). An enol or enolate of LGE_2, generated as depicted in **5**, could also be an intermediate in the formation of Δ^9-LGE_2. The pH and buffer dependence of these parallel first-order dehydration and allylic rearrangement reactions is presented in Figure 2. Since dehydration of **3** could generate $AnLGE_2$ (**2**), the possibility was considered that **3** is an intermediate in the production of $AnLGE_2$ from LGE_2. Control experiments (in 0.1 M aqueous pH 7.8 sodium phosphate buffer, see the Experimental Section) established that the decomposition of Δ^9-LGE_2 (**3**) is *much slower* than the dehydration of LGE_2 (see the Experimental Section). Therefore, the majority of $AnLGE_2$ must be produced directly from LGE_2 without the involvement of **3**.

Particularly noteworthy is the formation of Δ^9-LGE_2 (**3**) above pH 5.5. The possibility that the phosphate buffer catalyzes the decomposition of LGE_2 was examined. The observed rate constant for disappearance of LGE_2 shows a good linear correlation (R^2 = 0.980) with buffer concentration (Figure 3). The rate in 0.1 M phosphate is only slightly increased in the presence of 1.0 M NaCl, showing that the ionic strength of the medium is not a major factor determining the rate of LGE_2 decomposition. A similar insensitivity to ionic strength was noted previously for the

(6) Thompson, G. F.; Collins, J. M.; Schmalzried, L. M. *J. Pharm. Sci.* **1973**, *62*, 1738.
(7) Stehle, R. G. *Meth. Enzymol.* **1982**, *86*, 436.
(8) Stehle, R. G.; Smith, R. W. *J. Pharm. Sci.* **1976**, *65*, 1845.

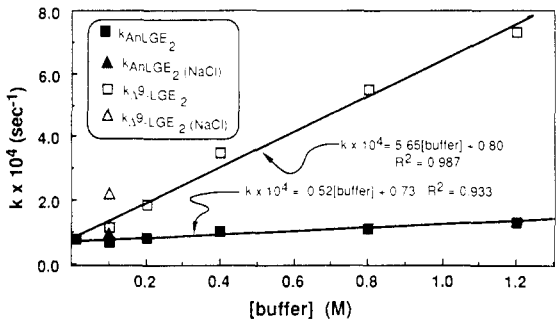

Figure 4. Rate constants for appearance of $AnLGE_2$ (**2**) and Δ^9-LGE_2 (**3**) as a function of pH 7.75 ± 0.05 phosphate buffer concentration at 37 °C.

decomposition of PGE_2 in aqueous solution.[8]

Since much less allylic rearrangement giving **3** seemed to occur in 0.01 M rather than in 0.1 M buffer, the possibility that the phosphate buffer catalyzes allylic rearrangement more strongly than it catalyzes dehydration was examined. Indeed, the pseudo-first-order rate constant for generation of **3** from LGE_2 is strongly linearly dependent on the molarity of the sodium phosphate buffer with $k_{\Delta^9\text{-}LGE_2} = 5.65[\text{buffer}] + 0.80$ (Figure 4). But the pseudo-first-order rate constant for generation of **2** from LGE_2 is only weakly dependent on the molarity of the sodium phosphate buffer with $k_{AnLGE_2} = 0.52[\text{buffer}] + 0.73$ (Figure 4).

To examine the influence of ionic strength on the pseudo-first-order rate constants for appearance of products, the reaction in 0.1 M pH 7.75 phosphate buffer was repeated in the presence of 1.0 M NaCl (see Figure 4). Small increases were observed in rate of appearance of $AnLGE_2$ and Δ^9-LGE_2 with an increase in the ionic strength of the medium. The small increase observed in the rate of appearance of $AnLGE_2$ with increasing buffer concentration may simply be the consequence of increasing ionic strength. However, increasing ionic strength of the medium cannot account for the large increase in the rate of allylic rearrangement of LGE_2 with increasing buffer concentration. Thus, in contrast with the dehydration of LGE_2 producing $AnLGE_2$ and with the dehydration of PGE_2[6] producing PGA_2, *the allylic rearrangement of* LGE_2 *producing* Δ^9-LGE_2 *is catalyzed by phosphate.* The three pK_a values for H_3PO_4 are 2.12, 7.21, and 12.32, respectively.[9] The predominant species between pH 5.5 and 8.0 are thus $H_2PO_4^-$ and HPO_4^{2-}. Both of these ions are not only capable of proton acceptance but also of proton donation. Therefore, catalysis might involve a rate-determining bifunctional proton abstraction α to the carbonyl with concomitant protonation of the aldehyde carbonyl oxygen leading to enolization as shown in the **6** to **7** conversion. Subsequent rapid protonation of the enol tautomer **7** of Δ^9-LGE_2 (**3**) at the 11 position and proton loss from oxygen would deliver the conjugated aldehyde **3**. Catalysis of enolization by phosphate is well known.[10]

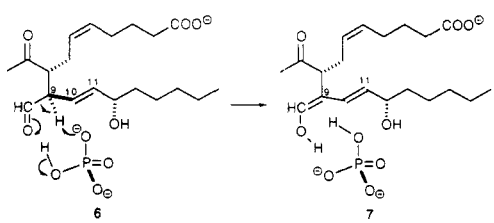

6 7

The present study demonstrates that LGE_2 readily undergoes dehydration and allylic rearrangement reactions in aqueous solutions at physiological pHs. However, these reactions are much slower than the reaction of LGE_2 with proteins to form covalent adducts.[15] Nevertheless, in view of the susceptibility of the allylic rearrangement to catalysis by phosphate and the likely existence of other catalysts for this reaction, the possibility that LGE_2 is transformed to rearrangement products under certain physiological conditions must be considered during evaluation of the biological actions of this levuglandin.

The exceptional stability of LGE_2 under mildly acidic conditions (pH 3–4) is especially important for our total synthesis[1] which involves cleavage of a vicinal diol precursor in aqueous acetic acid. The discovery that phosphate ions catalyze allylic prototropic rearrangement of LGE_2 generating Δ^9-LGE_2 provides a synthetically useful route to either this isomer or the dehydration product, $AnLGE_2$, by appropriate adjustment of buffer concentration.

Experimental Section

General. Proton nuclear magnetic resonance (NMR) spectra were recorded either on a Varian XL-200 spectrometer operating at 200.06 MHz or on a Bruker 400 MSL spectrometer operating at 400.130 MHz. Proton chemical shifts are reported in parts per million on the δ scale relative to tetramethylsilane (δ 0.00). Tetramethylsilane or residual chloroform (δ 7.24) were used as internal standards. Significant ^{1}H NMR spectral data are tabulated in order: multiplicity (s, singlet; d, doublet; t, triplet; q, quartet; m, multiplet; br, broad), number of protons, coupling constant(s) in hertz, and positional assignment if established. The use of apparent in proton multiplicity descriptions implies a hyperfine splitting necessarily more complex than first order. All NMR samples were analyzed as solutions in $CDCl_3$.

^{13}C NMR spectra were recorded either on a Varian XL-200 spectrometer operating at 50.31 MHz or on a Bruker 400 MSL spectrometer operating at 100.627 MHz. ^{13}C NMR are reported in parts per million on the δ scale relative to chloroform-*d* (δ 77.0). Attached proton test (APT)[11] spectra for ^{13}C were obtained using a Bruker 400 MSL spectrometer operating with the pulse sequence [D1–(90° pulse)–D2–(180° pulse)–(D2 + D3)–(180° pulse)–D3–data acquisition], where D1, D2, and D3 are delays equal to 7 s, 7 ms, and 40 μs, respectively. The high power proton decoupler was gated off during the first D2 delay and was on during the remainder of the pulse sequence. Under these conditions quaternary and methylene carbons exhibit phases opposite to those displayed by methine and methyl carbons. APT spectral phasing was adjusted such that quaternary and methylene carbons showed positive absorptions while methine and methyl carbons showed

(9) Bjerrum, J.; Schwarzenbach, G.; Sillen, L. G. *Stability Constants of Metal-Ion Complexes, Inorganic Ligands, Part II*; Chemical Society: London, 1957.

(10) (a) Burgner, J. W., II; Ray, W. J., Jr. *Biochemistry* **1974**, *13*, 4229. (b) Gallardo, H.; Guillo, L. A.; Duran, N.; Cilento, G. *Biochim. Biophys. Acta* **1984**, *789*, 57. (c) Thornalley, P.; Wolff, S.; Crabbe, J.; Stern, A. *Biophys. Acta* **1984**, *797*, 276. (d) Bohne, C.; MacDonald, I. D.; Dunford, H. B. *J. Biol. Chem.* **1987**, *262*, 3572.

(11) Patt, S. L.; Shoolery, J. N. *J. Magn. Reson.* **1982**, *46*, 535.

(12) (a) Cooper, G. F.; Fried, J. *Proc. Natl. Acad. Sci. U.S.A.* **1973**, *70*, 1579. (b) Conover, W. W.; Fried, J. *Proc. Natl. Acad. Sci. U.S.A.* **1974**, *71*, 2157. (c) Lukacs, G.; Piriou, F.; Gero, S. D.; Van Dorp, D. A. *Tetrahedron Lett.* **1973**, 515. (d) Hagen, R.; Roberts, J. D. *J. Am. Chem. Soc.* **1969**, *91*, 4504.

(13) A minimum value purity of LGE_2 (**1**) was determined by dividing the integral height of the aldehydic resonance by the integral height corresponding to one proton of the terminal methyl resonance (v 0.85, t, 3 H) and multiplying by 100. To insure quantitative integration of the aldehyde resonance, the T_1 relaxation of this resonance was determined by the inversion–recovery technique. Data analysis was performed using the standard Varian XL-200 T_1 software program. For LGE_2-methyl ester in $CDCl_3$ at 20 °C the T_1 relaxation of the aldehyde signal (s, δ 9.46) is 2.2 s. A pulse sequence delay of at least 5 times the calculated T_1 for a particular pulse width was used during data acquisition of spectra used for purity determinations.

(14) Colowick, S. P.; Kaplan, N. O. *Methods Enzymol.* **1955**, *1*, 143.

(15) Salomon, R. G.; Jirousek, M. R.; Ghosh, S.; Sharma, R. B. *Prostaglandins* **1987**, *34*, 643.

Table I. Citrate–Phosphate Buffers[a]

pH		citric acid		
calcd	found	wt, g	mmol	phos/cit
2.8	2.79	2.600	13.5	0.37
3.8	3.82	0.876	4.56	1.10
4.2	4.21	0.685	3.57	1.40
4.6	4.65	0.550	2.87	1.74
4.8	4.93	0.484	2.52	1.97
5.2	5.21	0.419	2.18	2.29
5.4	5.49	0.383	2.00	2.51

[a] Solid citric acid (the amounts indicated above) was dissolved in aqueous 0.2 M dibasic sodium phosphate (25.0 mL), and the resulting solution was diluted to a final volume of 50.0 mL.

negative absorptions. The results from APT spectra are shown by placing a plus (+) sign, indicating a quaternary or methylene carbon, or a minus (–) sign, indicating a methine or methyl carbon, after the chemical shift position of the carbon resonance. Assignments of carbon resonances were made on the basis of results from ATP spectra and by comparisons with published chemical shift data for related compounds.[12]

High-resolution mass spectra were recorded on a Kratos Analytical MS25RFA mass spectrometer. Samples were introduced to the ionization chamber by direct probe insertion. UV spectra were recorded on a Perkin-Elmer Model lambda-3 spectrophotometer. Optical rotatory dispersion (ORD) spectra were recorded on a Cary 60 spectrophotometer.

Thin-layer chromatography (TLC) was performed on precoated silica gel plates supplied by E. Merck, R_f values are quoted for plates of thickness 0.25 mm. Visualization was done by viewing the developed plates under short-wavelength UV light and by heating the plates after spraying with vanillin–sulfuric acid. Flash column chromatography was performed on 230–400-mesh silica gel supplied by E. Merck. Preparative high-pressure liquid chromatography (HPLC) was performed using a Waters Associates system consisting of a Waters M-6000A solvent delivery system and a Waters U6K injector. The eluate was monitored with a Waters R-401 differential refractometer or an Instrumentation Specialties Company Model 1840 UV absorbance detector.

The pH of the buffer solutions was measured at room temperature using a radiometer PHM84 research pH meter (Rainin Instruments Co., Inc., Woburn, MA). The pH meter was calibrated in the desired range using standard buffer solutions of pH 7, and pH 4 or 10. UV spectra were recorded using matched (far-UV) quartz cells of 10-mm path length (Markson Science Inc., Phoenix, AZ). Kinetic studies were performed by monitoring UV absorptivities. UV spectra were recorded on a Cary 2300 UV–visible–NIR spectrophotometer (Varian Techtron Pfy. limited, Mulgrave, Australia) using a Cary 2200/2300 DS-15 multiscan program. Kinetics data were processed using a Varian 2200/2300 series /DS-15 kinetics storage program and a Varian Cary series/DS-15 kinetics calculation program (enhanced version). For all experiments, the sample holder as well as the sample, were kept at a constant temperature of 37 ± 0.5 °C, using a cryostat.

Materials. All reactions were performed in an inert moisture-free atmosphere under a positive pressure of nitrogen or argon except when working in aqueous media. Purification and handling of all solvents and reagents used in synthetic procedures were conducted under a nitrogen or argon atmosphere except for aqueous solutions. All solvents were reagent grade or purer. Ethyl acetate, hexane, and diethyl ether used for extractions or chromatography were distilled to remove nonvolatile impurities prior to use. Water used in reactions was purified by passage through a reverse osmosis membrane to remove organic and particulate matter followed by distillation under nitrogen with partial condensation. Sodium metaperiodate was obtained from Aldrich Chemical Co., Inc., and was used without further purification. ACS grade monobasic sodium phosphate, dibasic sodium phosphate, citric acid, and standard buffer solutions were all obtained from Fisher Scientific Co. Levuglandin E_2 (LGE_2) was synthesized as described previously.[1]

Buffer Solutions. Sodium phosphate pH 5.7–8.0 buffers were prepared according to published procedures.[14] Citrate phosphate pH 2.8–5.4 buffers were prepared by modifying the method outlined in ref 14 such that all buffers were 0.1 M in dibasic sodium phosphate (see Table I). Addition of NaCl (1.0 M final concentration) to the standard recipe for 0.1 M pH 7.8 sodium phosphate buffer afforded a buffer of measured pH 7.30. To correct this effect of the ionic strength of the medium, an apparent pK_a, pK_a(apparent) = 6.268, was calculated using the expression: pH(measured) = pK_a(apparent) + log $[Na_2HPO_4]/[NaH_2PO_4]$. This value, which differs considerably from the pK_a = 7.210 in the absence of NaCl, was then used in the above expression to calculate a buffer composition for pH 7.8, i.e. 7.8 = 6.27 + log $[Na_2HPO_4]/[NaH_2PO_4]$, and the amounts of each phosphate salt needed were then calcualted using $[Na_2HPO_4]$ + $[NaH_2PO_4]$ = 0.1 M. The measured pH of the resulting buffer containing 1.0 M NaCl was 7.77.

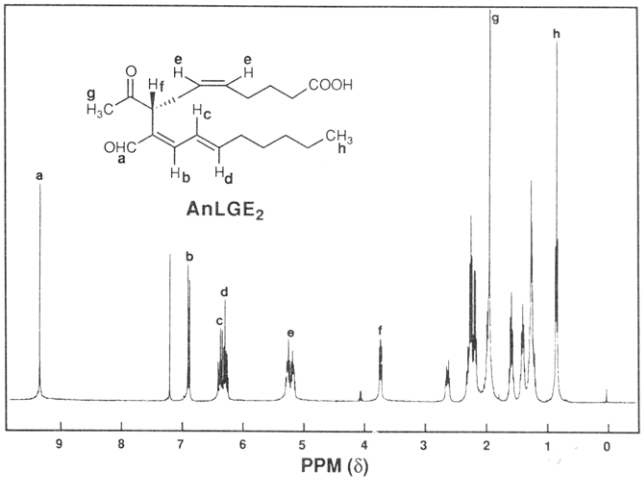

Figure 5. 400-MHz ^1H NMR spectrum of $AnLGE_2$ (**2**).

8-Acetyl-9-formyl-5(*Z*),9(*E*),11(*E*)-heptadecatrienoic Acid ($AnLGE_2$, 2). Synthetic LGE_2 (**1**) (10 mg, 65% aldehydic product,[13] 0.018 mmol) was dissolved in 0.01 M sodium phosphate pH 7.8 buffer[14] (100 mL) containing acetone (10 mL). The solution was stirred at room temperature for 48 h and then acidified with 2 N aqueous HCl to pH 3 and extracted with diethyl ether (4 × 30 mL). The combined organic extracts were dried ($MgSO_4$), filtered, and concentrated under reduced pressure to afford 10 mg of a yellow oil. This oil was purified by HPLC on a Whatman partisil column (4.6 mm i.d. × 20 cm) employing ethyl acetate/hexane (3:7, v/v) as the mobile phase at a flow of 0.6 mL/min. The eluate was monitored by UV detection at 320 nm. The retention time for $AnLGE_2$ (**2**) under these conditions was 16.2 min. After complete removal of solvents under reduced pressure there was obtained 5.3 mg (86% yield) of **10** as a clear oil: ^1H NMR (400.130 MHz, Figure 5) δ 9.39 (d, H, J = 0.6 Hz, CHO), 6.93 (d, H, J = 10.7 Hz, C-10 H), 6.49–6.22 (2 H, C-11, C-12 H's), 5.38–5.12 (2 H, C-5, C-6 H's), 3.78 (dd, H, J = 9.2, 5.7 Hz, C-8 H), 2.69–2.58 (m, H, C-7 H_a), 2.40–2.16 (3 H, C-7 H_b, C-13 H), 2.28 (t, 2 H, J = 7.6 Hz, C-2 H), 2.00 (apparent q, 2 H, J = 7.5 Hz, C-4 H), 1.98 (s, 3 H, acetyl methyl), 1.61 (apparent quintet, 2 H, J = 7.2 Hz, C-3 H), 1.50–1.31 (2 H, C-14 H), 1.35–1.15 (4 H, C-15, C-16 H's), 0.87 (t, 3 H, J = 6.7 Hz, C-17 H); ^{13}C NMR (100.627 MHz, $CDCl_3$) δ 206.69 (ketone carbonyl, +), 193.41 (aldehyde carbonyl, –), 178.41 (carboxylic acid carbonyl, +), 152.28 (–), 149.87 (–), 136.67 (C-9, +), 130.41 (–), 127.53 (–), 125.07 (–), 49.26 (C-8, –), 33.43 (+), 33.20 (+), 31.33 (+), 28.23 (two coincident resonances, + and –), 26.95 (+), 26.47 (+), 24.51 (+), 22.40 (+), 13.95 (–); UV (c 3.6 × 10^{-5}, $CDCl_3$), λ_{max}^{287} (ε = 20 900); high-resolution mass spectrum, m/e calculated for $C_{20}H_{30}O_4$, 334.2147, found m/e (rel intensity) 334.2126 (0.5), 316 (0.6), 219 (1.0), 273 (2.0), 263 (2.7), 245 (0.9), 217 (1.6), 207 (2.0), 179 (2.3), 127 (1.5), 71 (8.0), 43 (100).

8(*R*)-Acetyl-9-formyl-12(*S*)-hydroxy-5(*Z*),9(*E*)-heptadecadienoic Acid (Δ^9-LGE_2, 3). Synthetic LGE_2 (**1**) (21 mg, 65% aldehydic product by ^1H NMR analysis[13] was dissolved in 0.1 M sodium phosphate pH 7.8 buffer[14] (50 mL) containing acetone (5 mL) and stirred for 48 h at room temperature. The solution was acidified to pH 3 with 2 M HCl and extracted with diethyl ether (3 × 20 mL). The combined organic extracts were dried ($MgSO_4$), filtered, and concentrated under reduced pressure to afford 23.5 mg of a pale yellow oil. This oil was dissolved in a

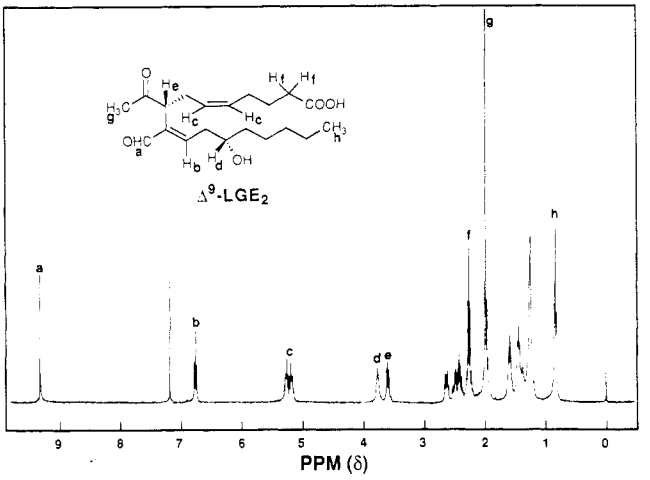

Figure 6. 400-MHz ^{1}H NMR spectrum of Δ^9-LGE_2 (**3**).

minimum amount of methylene chloride and streaked along the edge of a 0.25-mm silica gel TLC plate, and the plate was eluted twice with ethyl acetate/*n*-heptane/acetic acid (50:48:2, v/v/v). The two major UV absorbing bands at R_f's 0.67 (9.4 mg) and 0.43 (8.6 mg) were removed, the products each separately eluted from the silica gel with diethyl ether, concentrated under reduced pressure, and examined by ^{1}H NMR spectroscopy. The compound at R_f 0.67 was identified as $AnLGE_2$ while the compound at R_f 0.43 was the product resulting from double-bond isomerization. This latter product was further purified by HPLC on a Whatman Partisil column (4.6 mm i.d. × 25 cm) employing ethyl acetate-/*n*-heptane/acetic acid (40:58:2, v/v/v) as the mobile phase at a flow of 0.8 mL/min. Samples containing ca. 3 mg in 100 μL of the mobile phase were injected onto the column. Under these conditions, the retention time of Δ^9-LGE_2 was 15.5 min. The product was collected and the solvents were completely removed under reduced pressure to afford 8.2 mg of **3** as a clear colorless oil: ^{1}H NMR (400.130 MHz, $CDCl_3$, Figure 6) δ 9.39 (s, H, CHO), 6.82 (t, H, J = 7.5 Hz, C-10 H), 5.41–5.11 (2 H, C-5, C-6 H), 4.60–3.80 (br, 2 H, OH, COOH), 3.78 (m, H, J = 6.0 Hz, C-12 H), 3.60 (dd, H, J = 5.6, 9.1 Hz, C-8 H), 2.77–2.59 (m, H, C-7 H_a), 2.47 (dd, 2 H, J = 7.5, 6.1 Hz, C-11 H), 2.50–2.32 (m, H, C-7 H_b), 2.30 (t, 2 H, J = 7.2 Hz, C-2 H), 2.04 (s, 3 H, acetyl methyl), 2.01 (apparent q, 2 H, J = 7.2 Hz, C-4 H), 1.62 (apparent quintet, 2 H, J = 7.2 Hz, C-3) 1.56–1.39 (2 H, C-13 H), 1.28 (br s, 6 H, C-14, C-15, C-16 H), 0.87 (t, 3 H, J = 6.5 Hz, C-17 H); ^{13}C NMR (100.627 MHz, $CDCl_3$) δ 206.73 (ketone carbonyl), 193.68 (aldehyde carbonyl), 177.92 (carboxylic acid carbonyl), 154.70, 142.31 (C-9), 130.60, 1127.58, 70.94 (C-12), 49.53 (C-8), 37.51, 36.88, 33.11, 31.70, 28.32, 26.64, 26.45, 25.32, 24.49, 22.57, 13.97 (C-17); high-resolution mass spectrum, m/e calculated for $C_{20}H_{32}O_5$ 352.2249, found m/e (rel intensity) 352.2239 (0.1), 334 (0.6), 316 (0.4), 291 (1.4), 273 (1.6), 263 (1.7), 191 (4.3), 165 (4.3), 95 (9.1), 91 (11.9), 71 (7.0), 43 (100); UV (c 1.0 × 10-4, hexane) $\lambda_{max}^{215.5}$ nm (ϵ = 6000) (c 1.0 × 10^{-4}, 0.1 M sodium phosphate buffer, pH 7.8) $\lambda_{max}^{232.3}$ nm (ϵ = 11 570); ORD (c 3.5 × 10^{-3} g/100 mL, hexane) $[\alpha]_{309}$ +51°, $[\alpha]_{248}$ −69°, $[\alpha]_{212}$ 103°, $[\alpha]_{203}$ −160°.

Decomposition of LGE_2 in Aqueous Buffer Solutions at 37 °C. In 0.1 M pH 7.8 phosphate buffer at 37 °C, An-LGE_2 shows λ_{max} = 292 nm; ϵ_{292nm} = 27 500 and ϵ_{232nm} = 2225 while Δ^9-LGE_2 shows λ_{max} = 232 nm; ϵ_{232nm} = 6500 and ϵ_{292nm} = 415. At the concentrations of LGE_2 used in the kinetics experiments, LGE_2 itself does not absorb in this region of the UV. Therefore, since the anhydro and Δ^9 forms of LGE_2 are highly UV active, their rates of formation could be followed with ease. In a typical experiment, 5 μL of a stock solution of LGE_2 in CD_2Cl_2 (containing 20 mg of LGE_2/1.0 mL of CD_2Cl_2), was placed in the UV cell. Excess solvent was removed under a stream of nitrogen. The residue was then dissolved in approximately 3.0 mL of 0.1 M phosphate buffer pH = 7.8 (maintained at 37 °C). The cell was capped and quickly placed in the sample holder (also maintained at 37 °C), and the UV spectra were recorded using the Cary multiscan program. The progress of the reaction was continuously monitored by recording the spectra at regular time intervals from the start of the reaction to a stage where no significant change in absorbance could be detected (at least 5 half-lives). Absorbance data (232 and 292 nm) were fed into the Cary kinetics calculation program which uses a Taylor's series algorithm to converge on optimal values of A_∞ (the end point of the reaction) and the pseudo-first-order rate constant (based on initial operator estimates). The decomposition of LGE_2 in phosphate buffers at 37 °C exhibits parallel first-order kinetics. As the buffer is used in a very large excess relative to LGE_2 concentration, the reaction is assumed to be a pseudo-first-order process. Prior to determining the product composition of the reaction mixture (at the end point of the reaction), we determined product stabilities in the same buffer under identical reaction conditions. Thus at 38 °C, in 0.1 M phosphate buffer pH 7.8, 5.5% of initially added $AnLGE_2$ decomposed (to unidentified products) over 70 h; under identical conditions, about 12% of the Δ^9-LGE_2 decomposed over 70 h at 38 °C; part of this being slowly converted to $AnLGE_2$. When the reaction was carried out at 50 °C in 0.1 M phosphate buffer pH 7.8, about 25% of $AnLGE_2$ decomposed over 100 h while 32% of Δ^9-LGE_2 decomposed; about $^1/_3$ of the Δ^9-LGE_2 was converted to $AnLGE_2$. As the thermal decomposition of $AnLGE_2$ and the conversion of Δ^9-LGE_2 to $AnLGE_2$, is slow relative to the formation of these products (from LGE_2), these secondary reactions were excluded from the kinetic scheme. Thus, the rate constant obtained from the two wavelengths of interest (292 and 232 nm) were averaged to get observed pseudo-first-order rate constant (k_{obs}). The individual rate constants k_{An} and k_{Δ^9} were obtained from k_{obs} and the mole ratio of products using the equations:

$$k_{obs} = k_{An} + k_{\Delta^9}$$

$$k_{An}/k_{\Delta^9} = [AnLGE_2]/[\Delta^9\text{-}LGE_2]$$

The results from decomposition of LGE_2 in 0.1 M phosphate buffers at 37 °C, over a range of pH values is shown in Figure 1. To access pH values in the range pH 2.8–4.8, 0.1 M citrate–phosphate buffers were used.

Acknowledgment. This research was supported by NIH Grant GM21249-12. We thank Professor Garnett R. McMillan for helpful discussions.

Registry No. **1**, 91712-41-3; **2**, 121843-91-2; **3**, 111219-91-1.